Supplementary Information

Supplementary Figures

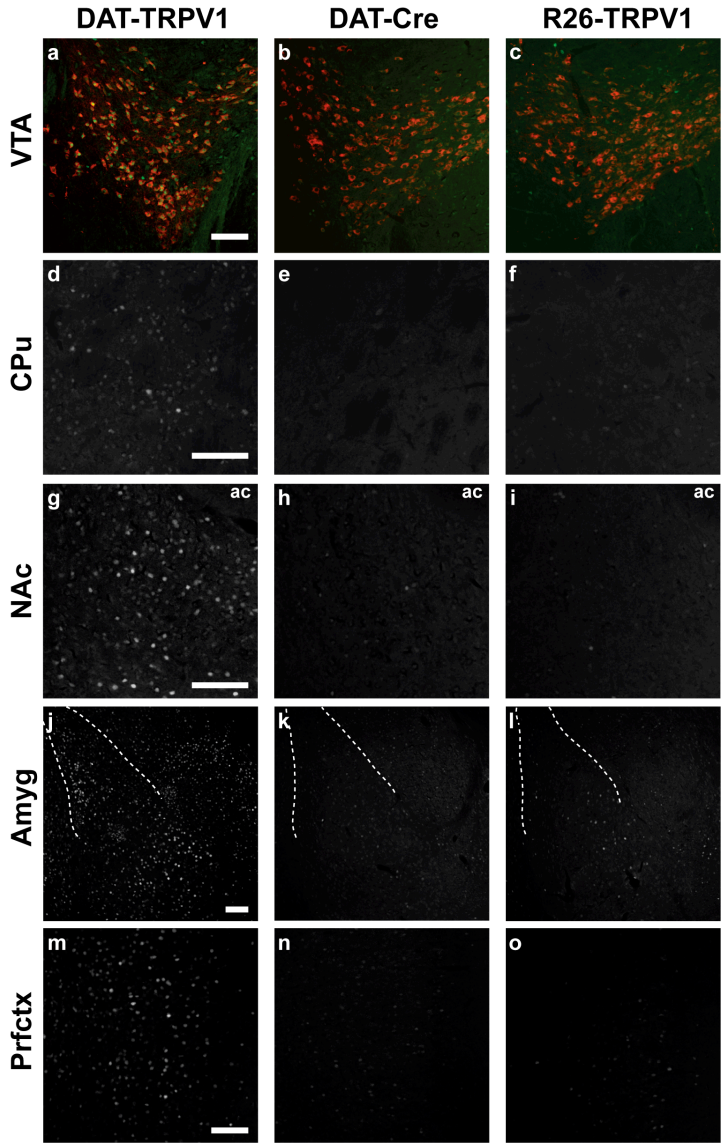

Supplementary Figure S1: Capsaicin induced c-Fos expression in DA cells and their targets. (a-c) Pseudo-colored images from double fluorescent immunohistochemistry with TH (red) and c-Fos (green) antibody in midbrain 90

min after capsaicin injection (32 mg/kg) of DAT-TRPV1 (a), DAT-Cre (b) or R26-TRPV1 (c) mice. Only 0.8±0.5 % and 0.5±0.3 % of TH positive cells were also c-Fos positive in DAT-Cre and Rosa26-TRPV1, respectively. **(d-o)** Fluorescent immunohistochemistry with c-Fos antibody of caudate putamen (CPu; d-f), nucleus accumbens (NAc; g-i), amygdala (Amyg; j-l), prefrontal cortex (Prfctx; M-O) 90 min after capsaicin injection (32 mg/kg) of DAT-TRPV1, DAT-Cre or R26-TRPV1 mice (ac: anterior commissure). All scale bars are 100 µm.

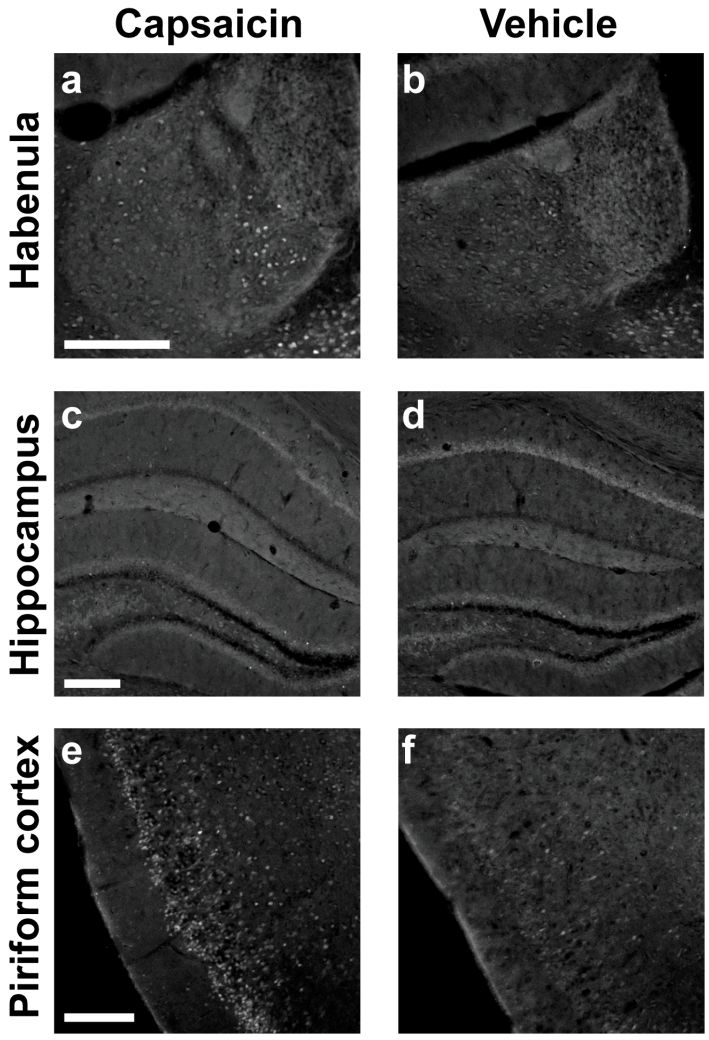

Supplementary Figure S2: c-Fos expression in some DA cells target regions following capsaicin administration. (a-f) Fluorescent immunohistochemistry with c-Fos antibody of habenula (a-b), hippocampus (c-d), piriformcortex (e-f) 90 min after capsaicin (32 mg/kg; left) or vehicle (right) injection of DAT-TRPV1 mice. All scale bars are 200 μm.

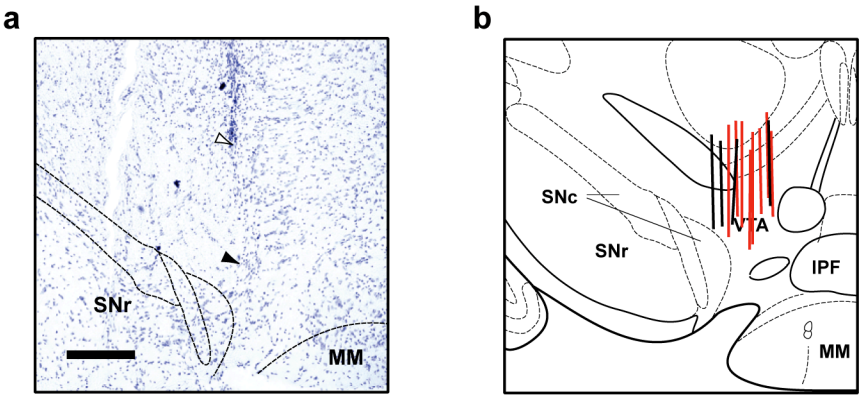

Supplementary Figure S3: Tetrode targeting for *in vivo* electrophysiology.

(a) Sample cresyl–violet staining to identify tetrode tracks (open arrowhead: end of guide tubing track mark; filled arrow head: end of tetrode track mark). **(b)** Representation of tetrode tracks on ventral midbrain; illustration adapted from Paxinos and Franklin Mouse Brain Atlas (Control: black; DAT-TRPV1: red). MM: mammillary nucleus, IPF: interpeduncular fossa, SNr: reticular substantia nigra. Scale bar is 200 μm.

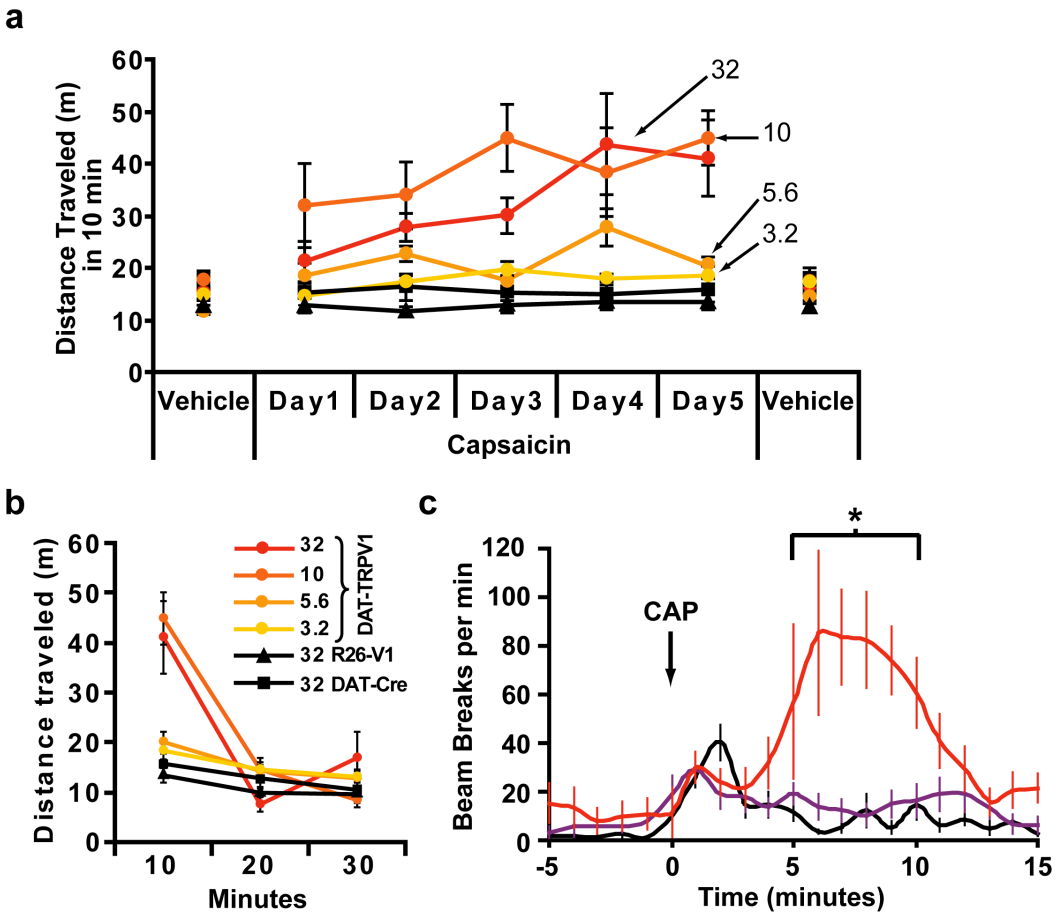

Supplementary Figure S4: Capsaicin induced locomotion. (a) Distance travelled in a novel environment by control and DAT-TRPV1 mice during initial 10 min after i.p. capsaicin injections for 5 consecutive days (n=7-10 per group). Mice were habituated to handling with vehicle injections three prior days. Responses to vehicle injections one day pre- and post-capsaicin days are plotted for comparison. DAT-TRPV1 mice injected with varying does of capsaicin as indicated (red: 32, dark-orange: 10, orange: 5.6, yellow: 3.2 mg/kg). R26-TRPV1 (black triangles) or DAT-Cre (black squares) control mice injected with vehicle or

capsaicin (32 mg/kg) as indicated (two-way repeated measures ANOVA: group effect, $F_{(5, 42)}$=16.48, p<0.0001). **(b)** Distance travelled plotted in 10 minute bins from (a) on day 5 following i.p. capsaicin injections. **(c)** Capsaicin (5.6 mg/kg; CAP; arrow indicates time of injection) induced activity monitored as number of beam-breaks per minute made by R26-TRPV1 (black), DAT-Cre (purple) or DAT-TRPV1 (red) mice (n=6-8 per group; two-way repeated measures ANOVA: group × time effect, F(40, 340)=5.59, p<0.0001; Bonferroni posttest, p<0.05:*). All error bars are ±SEM.

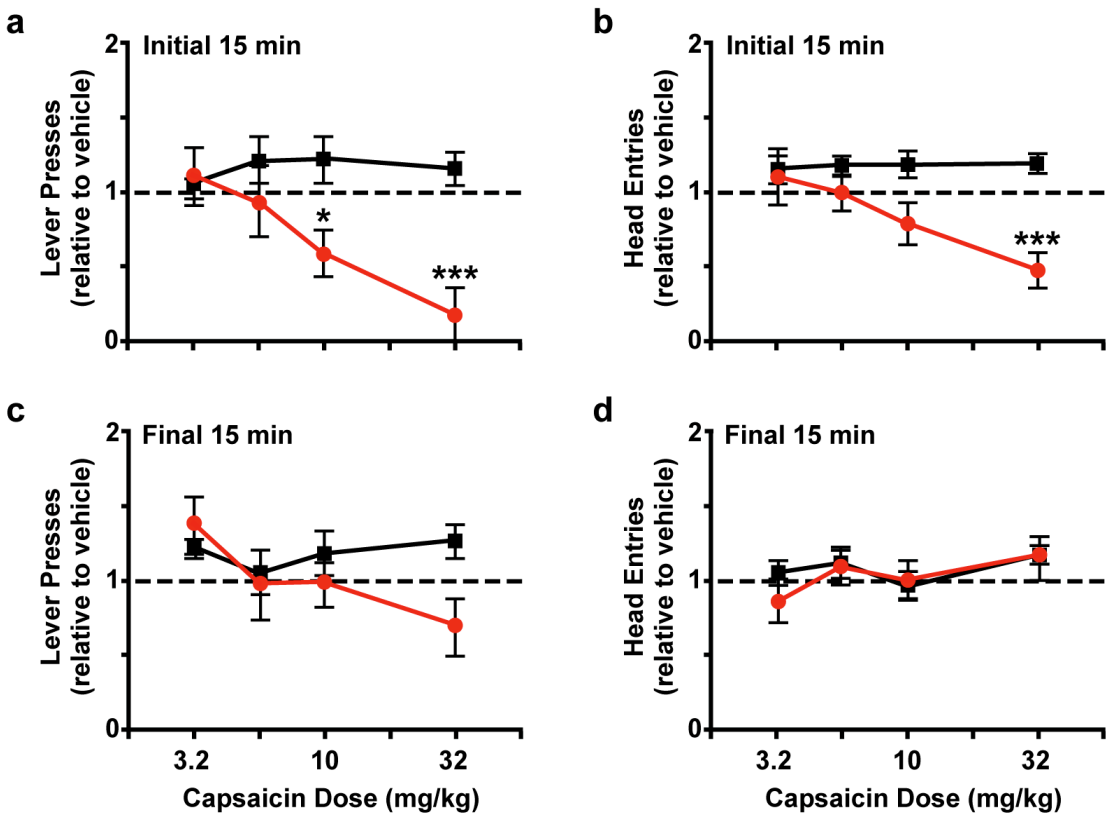

Supplementary Figure S5: Progressive-ratio responses upon capsaicin administration. (a-d) Normalized lever-presses (a and c) or head-entries (b and d) in PR made by control (black; n=14) or DAT-TRPV1 (red n=9) during initial (a and b) or final (c and d) 15 min of an hour-long session (two-way repeated measures ANOVA: group×dose effect for lever presses $F(3, 63) = 6.88$, $p = 0.0004$ and for head entries $F_{(3, 63)}=4.65$, $p=0.0053$. Bonferroni posttests, $p<0.05$:*, $p<0.001$:***). All error bars are ±SEM.

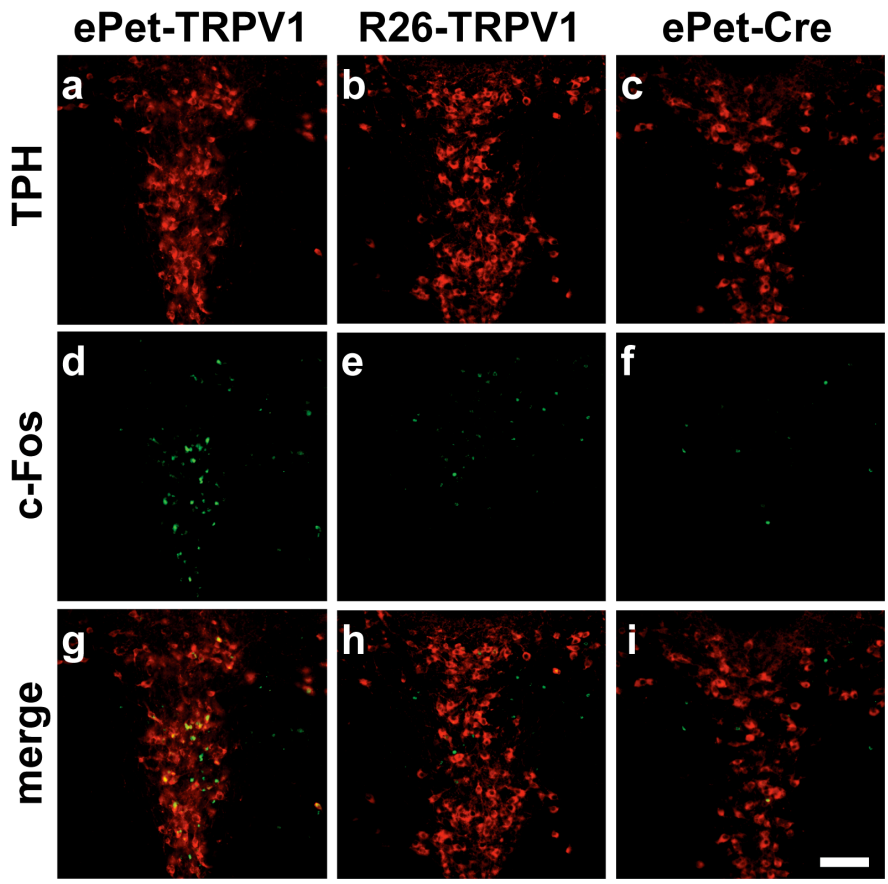

Supplementary Figure S6: Capsaicin induced c-Fos expression in serotonergic cells. (a-i) Double fluorescent immunohistochemistry with TPH (a-c) and c-Fos (d-f) antibody in the dorsal raphe 90 min after capsaicin injection (32 mg/kg) of ePet-TRPV1 (left), R26-TRPV1 (middle) or ePet-Cre (right) mice (Capsaicin-induced c-Fos expression in TPH expressing cells of ePet-TRPV1: 71.2±3.4 %, R26-TRPV1:14.4±4.2 % or ePet-Cre: 12.1±3.7 %; n=3 per group). Pseudo-colored images are merged in (g-i). Scale bar is 100 µm.

Supplementary Discussion

DAT-TRPV1 and ePet-TRPV1 mice

In DAT-TRPV1 and ePet-TRPV1 lines, we confirmed functional TRPV1 expression in the selected cell groups by capsaicin-induced increases in c-Fos protein, an indicator of increased neural activity. This was possible even though we were not able to detect TRPV1 expression directly with immunohistochemical methods (using three separate antibodies against TRPV1). Slice and *in vivo* electrophysiological experiments in DAT-TRPV1 mice confirm that capsaicin administration induces reversible neural excitation in the targeted cell groups. Furthermore, the FSCV recordings demonstrate this activity is converted to DA release which is the most likely culprit for the elevated c-Fos in the downstream targets. Taken together, our results suggest that inducible activity of TRPV1 is able to modulate neural activity of genetically targeted cell groups.

Both STEMA lines highlight the utility of this system as they recapitulate some of the well characterized behaviors of their respective pharmaceutical counterparts. For instance, DA agonists or DAT inhibitors that mimic increases in dopaminergic activity have been demonstrated to increase locomotion, modulate operant responding for food and *ad libidum* feeding similar to capsaicin administered DAT-TRPV1 mice[53-59]. However, the STEMA-induced behaviors are dissimilar in their temporal resolution to DA agonists or drugs that elevate dopaminergic tone (most of which have effects that last for hours). This pharmacodynamic difference most likely stems from the ability of capsaicin to robustly activate TRPV1 and then be metabolized within minutes [60,61]. The rapid

pharmacokinetics of capsaicin allows closely timed drug administrations to induce similar activity responses. This feature of STEMA is desirable in cases where fast neural activation and reversal to baseline is required. Furthermore, the bi-directional control of feeding behavior in DAT-TRPV1 mice highlights the precise control that can be achieved with STEMA.

The preference of DAT-TRPV1 mice for solution containing hot chili pepper extract demonstrates that elevation in dopaminergic cellular activity is sufficient to create incentive value for an otherwise noxious compound. The time period between ingestion of capsaicin and induced dopaminergic activity must be sufficiently close to allow association between the rewarding effects and the event that initiates it. In humans, orally consumed capsaicin can be detected in circulation within 10 min after which it is rapidly metabolized[60]. The ability of DAT-TRPV1 mice to develop a preference with repeated consumption events indicates similar pharmacokinetics and underscores the value of fast temporal dynamics in capsaicin-induced neural activation. Our findings are in alignment with other self-administration or -stimulation techniques that demonstrate rewarding effects of potentiated dopaminergic tone[62-64]. For instance, intracranial self-stimulation (ICSS) can be achieved by targeting either the VTA or MFB [65,67]. Moreover, phasic optogenetic stimulation of dopaminergic neurons is sufficient to elicit conditioned place preference, increase the consumption of sweetened water that is paired with it or preference for a lever associated with it during the acquisition of an appetitive operant conditioning task[65-67]. By demonstrating STEMA in DAT-expressing neurons is able to sustain oral self-administration of

capsaicin, we underscore sufficiency of induced dopaminergic activity for such behaviors.

Behavioral responses of STEMA in ePet-TRPV1 mouse model demonstrate adaptability of this system to any Cre line allowing ability to screen for physiological or behavioral responses with ease. Similar to some 5-HT agonists or acute high dose administration of selective serotonin reuptake inhibitors (SSRIs), we observed decreased activity at higher doses of capsaicin in ePet-TRPV1 mice[71,72]. More significantly, a dose that did not inhibit locomotion produced anxiogenic-like effect in the open-field test. This response is similar to the acute effects of SSRIs like fluoxetine and citalopram[68,69]. By combining pharmacological and transgenic techniques, ePet-TRPV1 offer unique advantages in examining role of serotonergic neurons not only in anxiety related behaviors but also other 5-HT modulated physiological responses.

Transgenic mouse models with constant elevated DA or 5-HT levels have yielded significant insights in the behavioral consequences of signaling dysregulation in these neurotransmitter systems[70-72]. DAT knock-out or knock-down mice with disrupted clearance of released DA display a wide range of abnormal behaviors from hyperactivity in a novel environment to cognitive inflexibility[70,71]. Similarly, serotonin transporter (SERT) knock-out animals exhibit marked increases in extracellular 5-HT levels and display a prominent anxiety-like phenotype[75,76]. However, life-long elevated extracellular DA or 5-HT levels in these mouse models lead to significant regulatory changes in neurotransmitter signaling and metabolism as well as cellular physiology[71]. Traditional

pharmaceuticals circumvent this caveat but allow potential unwanted off-target side-effects. Therefore, inducible effector systems, like STEMA, bring advantages in assessing behavioral correlates of neural signaling. This feature, coupled with the ability to genetically target TRPV1, makes STEMA a unique pharmacological tool allowing precise manipulation of genetically identified neural subtypes.

Future and possible advancements

It is possible to generate a variety of temporally distinct activation patterns by utilizing various types of selective TRPV1 agonists[77]. However, systemic ligand administration with STEMA is unlikely to achieve sub-second temporal resolution desirable for on/off kinetics at neuronal time scales. Millisecond activation might be accomplished with photoreleasble ligands of TRPV1[73]. With a pulse of ultraviolet light (5 msec) these ligands are photolysed to their active form allowing quick responses. Alternatively, taking advantage of thermosensitivity of capsaicin receptor, it maybe possible to selectively activate TRPV1 expressing neurons with a 100 msec flash of infrared light[74]. In either case, the light source can be delivered via fiber optic cable to the target site to achieve faster kinetics.

Supplementary Methods

Operant conditioning

For instrumental conditioning in mice, a computer equipped with the MED-PC IV program controlled standard sound-attenuated mouse operant chambers (model ENV-300, Med Associates) to record lever presses and head entries into the food hopper. In an hour long session, mice were pre-trained on a two-lever fixed ratio 1 (FR1) schedule of reinforcement for 7 days. Preferred lever was used for 3 additional days with FR5 schedule during 20-min sessions. Daily sessions of 1 hour single-lever progressive ratio (PR) testing was then conducted for 3 days followed by 3 days of PR testing after vehicle administration (i.p.) to habituate animals to injection[52]. For the last four PR sessions, mice were injected with capsaicin at 3.2, 10, 32 or 5.6 mg/kg of body weight just prior to session start. Total lever presses and head entries into the food hopper were recorded and analyzed in 15-min bins.

Supplementary References

52 Robinson, S., Rainwater, A. J., Hnasko, T. S. & Palmiter, R. D. Viral restoration of dopamine signaling to the dorsal striatum restores instrumental conditioning to dopamine-deficient mice. *Psychopharmacology (Berl)* **191**, 567-578 (2007).

53 Cannon, C. M., Abdallah, L., Tecott, L. H., During, M. J. & Palmiter, R. D. Dysregulation of striatal dopamine signaling by amphetamine inhibits feeding by hungry mice. *Neuron* **44**, 509-520 (2004).

54 Caul, W. F. & Brindle, N. A. Schedule-dependent effects of haloperidol and amphetamine: multiple-schedule task shows within-subject effects. *Pharmacol Biochem Behav* **68**, 53-63 (2001).

55 Evans, K. R. & Vaccarino, F. J. Effects of d- and l-amphetamine on food intake: evidence for a dopaminergic substrate. *Pharmacol Biochem Behav* **27**, 649-652 (1987).

56 Fossom, L. H. & Sparber, S. B. Potentiation by naltrexone of d-amphetamine-induced behavioral suppression and its reversal by clonidine. *Life Sci* **31**, 2827-2835 (1982).

57 O'Neill, M. F. & Shaw, G. Comparison of dopamine receptor antagonists on hyperlocomotion induced by cocaine, amphetamine, MK-801 and the dopamine D1 agonist C-APB in mice. *Psychopharmacology (Berl)* **145**, 237-250 (1999).

58 Peterson, D. W. & Sparber, S. B. Increased fixed-ratio performance and differential d- and l-amphetamine action following norepinephrine depletion by intraventricular 6-hydroxydopamine. *J Pharmacol Exp Ther* **191**, 349-357 (1974).

59 van der Hoek, G. A. & Cooper, S. J. The selective dopamine uptake inhibitor GBR 12909: its effects on the microstructure of feeding in rats. *Pharmacol Biochem Behav* **48**, 135-140 (1994).

60 Chaiyasit, K., Khovidhunkit, W. & Wittayalertpanya, S. Pharmacokinetic and the effect of capsaicin in Capsicum frutescens on decreasing plasma glucose level. *J Med Assoc Thai* **92**, 108-113 (2009).

61 Chanda, S., Bashir, M., Babbar, S., Koganti, A. & Bley, K. In vitro hepatic and skin metabolism of capsaicin. *Drug Metab Dispos* **36**, 670-675 (2008).

62 Carlezon, W. A., Jr. & Chartoff, E. H. Intracranial self-stimulation (ICSS) in rodents to study the neurobiology of motivation. *Nat Protoc* **2**, 2987-2995 (2007).

63 McBride, W. J., Murphy, J. M. & Ikemoto, S. Localization of brain reinforcement mechanisms: intracranial self-administration and intracranial place-conditioning studies. *Behav Brain Res* **101**, 129-152 (1999).

64 Owesson-White, C. A., Cheer, J. F., Beyene, M., Carelli, R. M. & Wightman, R. M. Dynamic changes in accumbens dopamine correlate with learning during intracranial self-stimulation. *Proc Natl Acad Sci USA* **105**, 11957-11962 (2008).

65 Adamantidis, A. R. *et al.* Optogenetic Interrogation of Dopaminergic Modulation of the Multiple Phases of Reward-Seeking Behavior. *J Neurosci* **31**, 10829-10835 (2011).
66 Domingos, A. I. *et al.* Leptin regulates the reward value of nutrient. *Nat Neurosci* **14**, 1562-1568 (2011).
67 Tsai, H. C. *et al.* Phasic firing in dopaminergic neurons is sufficient for behavioral conditioning. *Science* **324**, 1080-1084 (2009).
68 Birkett, M. A. *et al.* Acute anxiogenic-like effects of selective serotonin reuptake inhibitors are attenuated by the benzodiazepine diazepam in BALB/c mice. *Pharmacol Biochem Behav* **98**, 544-551 (2011).
69 Burghardt, N. S., Sullivan, G. M., McEwen, B. S., Gorman, J. M. & LeDoux, J. E. The selective serotonin reuptake inhibitor citalopram increases fear after acute treatment but reduces fear with chronic treatment: a comparison with tianeptine. *Biol Psychiatry* **55**, 1171-1178 (2004).
70 Gainetdinov, R. R. Dopamine transporter mutant mice in experimental neuropharmacology. *Naunyn Schmiedebergs Arch Pharmacol* **377**, 301-313 (2008).
71 Haenisch, B. & Bonisch, H. Depression and antidepressants: insights from knockout of dopamine, serotonin or noradrenaline re-uptake transporters. *Pharmacol Ther* **129**, 352-368 (2011).
72 Kalueff, A. V., Olivier, J. D., Nonkes, L. J. & Homberg, J. R. Conserved role for the serotonin transporter gene in rat and mouse neurobehavioral endophenotypes. *Neurosci Biobehav Rev* **34**, 373-386 (2010).
73 Zhao, J. *et al.* Caged vanilloid ligands for activation of TRPV1 receptors by 1- and 2-photon excitation. *Biochemistry* **45**, 4915-4926 (2006).
74 Tzabazis, A. Z. *et al.* Selective nociceptor activation in volunteers by infrared diode laser. *Mol Pain* **7**, 18 (2011).